ACADEMIA ROMÂNĂ
Revue Roumaine de Chimie
http://web.icf.ro/rrch/

Rev. Roum. Chim.,
2014, *59*(8), 683-691

PHOTOPHYSICAL PROPERTIES OF TWO DERIVATIVES IN THE PHENOXATHIIN-10,10-DIOXIDE CLASS

Mariana DUCA,[a] Iulia MATEI[a,b] and Mihaela HILLEBRAND[a,*]

[a] Department of Physical Chemistry, University of Bucharest, 4–12 Regina Elisabeta Bd., 030018 Bucharest, Roumania
[b] "Ilie Murgulescu" Institute of Physical Chemistry of the Romanian Academy, 202 Splaiul Independentei, Bucharest 060021, Roumania

Received April 30, 2014

The emission spectra of two phenoxathiin-10,10-dioxide derivatives, 3-CH_3- and 3-CH_2Br-substituted, were recorded and discussed. In passing from cyclohexane to polar protic solvents, the fluorescence spectrum of the bromine-substituted compound showed a strong solvent dependence reflected in the bathochromic shift of the peak and a broadening of the band. The solvatochromic effect was analyzed in terms of the Lippert-Mataga, Reinchardt and Kamlet-Taft models. For the first two models, a good linearity was found when neglecting the protic solvents. The parameters obtained using the Kamlet-Taft model showed quasi-similar contributions from the solvent hydrogen bond donor and acceptor properties. The isodensity contours of the frontier molecular orbitals involved in the first excited singlet state, obtained by TDDFT calculations, explain the experimental data by evidencing a charge transfer from the heteroring towards the substituent. The theoretical results also account for the spectral differences between the 3-CH_3 and 3-CH_2Br derivatives.

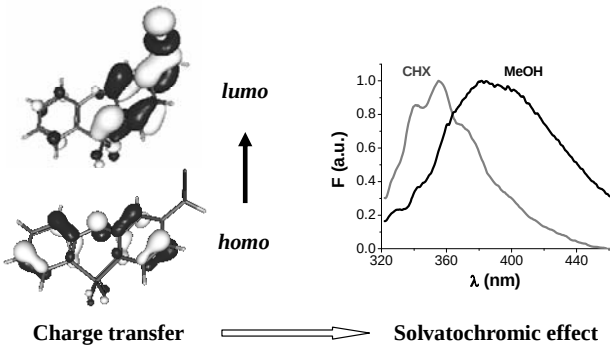

INTRODUCTION

Sulphur containing anthracene-like heterocycles are characterized by a pregnant donor character, experimentally manifested in the formation of donor−acceptor complexes and the stability of the cation radicals.[1–3] From the theoretical point of view, these properties are correlated with the preferential localization of the highest occupied molecular orbital (*homo*) on the sulphur atom. In some cases, the presence of a substituent on the different ring positions can modify the reactivity[4] and/or redox properties and favour the formation of both cationic and anionic radical species. In the excited state, these sulphur containing compounds present low fluorescence quantum yields due to an enhanced propensity for intersystem crossing deactivation. In the case of phenoxathiin derivatives, we have shown that the substituent nature and the ring substituted position can improve the emissive properties, the derivatives in position 3 of the ring possessing enhanced fluorescence emission.[5] This was explained by a change in the character of the first excited state determined by the nature of the lowest occupied molecular orbital (*lumo*); the greater localization of *lumo* on the substituent, the larger the expected fluorescence quantum yield.

* Corresponding author: mihh@gw-chimie.math.unibuc.ro

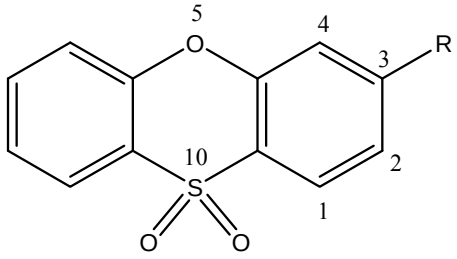

R
H (Phx-SO_2)
CH_3 (**I**)
CH_2Br (**II**)

Fig. 1 − Molecular structures of the investigated phenoxathiin-10,10-dioxide derivatives.

The oxidation of the sulphur atom to the corresponding sulphoxide and sulphone also brings about a change in the general behaviour and reactivity of the compounds.[6–9] In the followings, we wish to discuss the photophysical properties of two phenoxathiin-10,10-dioxide derivatives substituted in position 3 (Fig. 1, compounds **I** and **II**). Similar to the case of phenoxathiin derivatives, substitution in position 2 of phenoxathiinsulphone derivatives leads to low fluorescence quantum yields and unreliable emissive properties. We aim to determine the main features of the photophysical properties, *i.e.* the position of the fluorescence band in different solvents, the fluorescence quantum yield, and to discuss the overall effect of the sulphone group and substituent nature. It is well known that fluorophore sensitivity to solvents is of great interest for the analysis of emission spectra from fluorophores that are bound to proteins, membranes, nucleic acids and complex assemblies of macromolecules, given the importance of detecting fluorophore binding to macromolecules or of inferring the polarity of the binding site on the macromolecule.

RESULTS AND DISCUSSION

Photophysical parameters

Compounds **I** and **II** present an intense absorption band in the range 230−250 nm and a less intense one around 300 nm that we have used for excitation. The photophysical properties, wavelengths of the absorption and fluorescence maxima, and fluorescence quantum yields of the two compounds in methanol are presented in Table 1.

The first experimental observation was the large bathochromic shift of the fluorescence band generated by bromine substitution, as compared to the negligible effect of substitution on the absorption spectrum. To better evidence the spectral differences between the two derivatives and the large Stokes shift observed for **II**, its fluorescence spectrum was recorded in several solvents with different polarity and proticity. Some relevant results are displayed in Fig. 2 and Table 2. The spectra in Fig. 2 correspond to some representative solvents, namely cyclohexane (CHX) as nonpolar solvent, acetonitrile (ACN) as polar aprotic solvent and two protic solvents, 1-butanol (n-BuOH) and methanol (MeOH).

On going from CHX to MeOH one observes, besides the red shift of the fluorescence band, a significant increase in the spectral bandwidth, which lead us to suppose the presence of two bands, that is the presence in the system of two emitting species. The deconvolution of the fluorescence spectra in protic solvents (*e.g.* MeOH, inset of Fig. 2) shows indeed the presence of two bands located in the range 353−373 nm (λ_1) and around 400 nm (λ_2). The spectrum in CHX was also initially deconvoluted into two bands (inset of Fig. 2), but as this spectrum presents a vibrational structure, a better fit was obtained considering four bands in the range 320−380 nm (separated by about 1250 cm^{-1} and reflecting the vibrational structure) and a fifth band at 379 nm, with a larger width than the first four ones. In MeOH, the vibrational structure is not apparent and fitting with two bands was sufficient for matching well the experimental spectrum. The area of the long-wavelength band is greatly enhanced in MeOH as compared to CHX. Moreover, the ratio of the areas of the two bands, $A_{\lambda 2}/A_{\lambda 1}$, increases in MeOH as compared to ACN. The data resulting from the deconvolution analysis are shown in Table 3. As the dielectric constants of ACN and MeOH are not very different, we can assume that solvent polarity does not play the key role in favouring the species emitting at 400 nm. We tentatively assign this emission to a solvated species stabilized by hydrogen bond formation with the solvent, and therefore enhanced in protic media.

Table 1

Photophysical properties, wavelengths of absorption (λ_a) and fluorescence (λ_F) maxima, and fluorescence quantum yields (Φ) of the investigated compounds in methanol

Compound	λ_a (nm)	λ_F (nm)	Φ
I	292	313	0.05
II	296	381	0.04

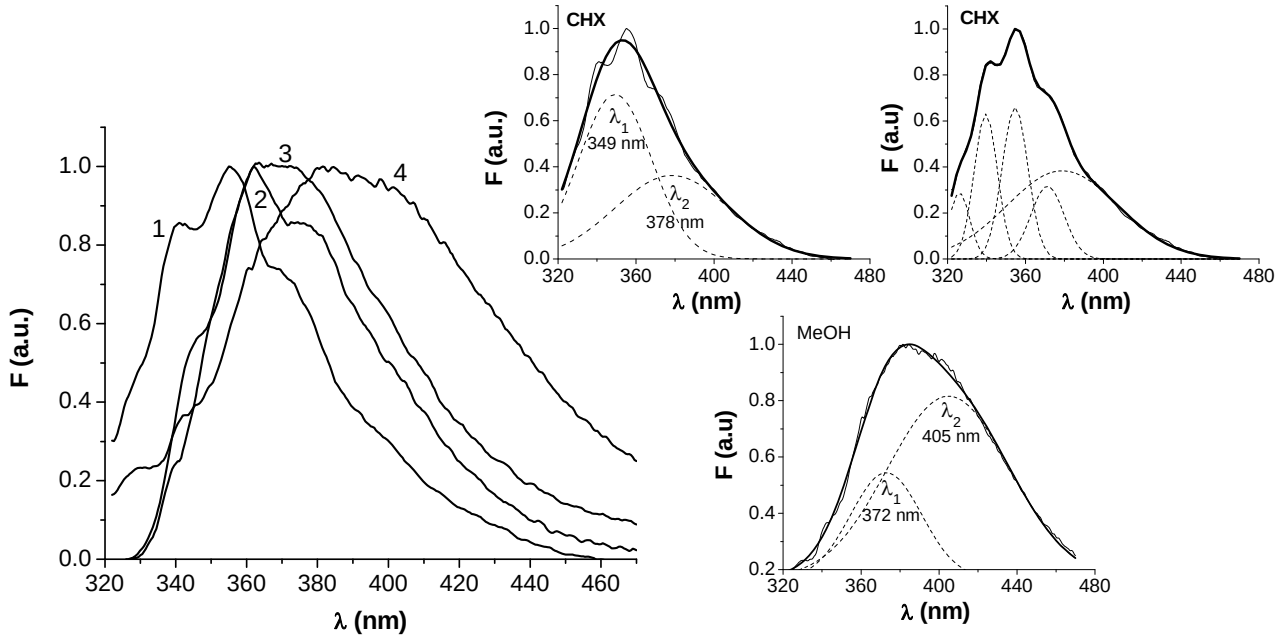

Fig. 2 − Normalized fluorescence spectra of **II** in different solvents (λ_{ex} = 296 nm): 1) CHX, 2) n-BuOH, 3) ACN, 4) MeOH. Inset: The deconvolution of the fluorescence band in CHX (two bands, $r^2 = 0.994$; five bands (see text), $r^2 = 0.999$) and MeOH (two bands, $r^2 = 0.997$).

Table 2

Relevant spectral information for compound **II** in different solvents*

Solvent	λ_a (nm)	λ_F (nm)	ν_F (cm^{-1})	$\Delta\nu_{Stokes}$ (cm^{-1})
CHX	296	355	28169	5615
HEX	292	355	28209	6038
$CHCl_3$	296	362	27624	6160
CH_2Cl_2	296	363	27586	6198
ACN	296	367	27248	6536
n-BuOH	296	359	27855	5929
EtOH	296	361	27701	6083
MeOH	296	383	26144	7640

* Solvent abbreviations: cyclohexane (CHX), hexane (HEX), acetonitrile (ACN), 1-butanol (n-BuOH), ethanol (EtOH) and methanol (MeOH).

Table 3

The two bands λ_1 and λ_2 resulting from the deconvolution of the emission band of compound **II** in nonpolar, polar aprotic and protic solvents, and the ratio of their areas ($A_{\lambda 2}/A_{\lambda 1}$)

Solvent	λ_1(nm)	λ_2(nm)	$A_{\lambda 2}/A_{\lambda 1}$
CHX	349.38	378.39	0.8
n-BuOH	352.98	393.17	1.4
MeOH	372.75	405.29	2.8
ACN	366.95	399.76	1.1

Several models have been used to analyze the experimentally observed solvatochromic effect for compound **II**, and shed light into the nature of the emitting species. The first model corresponds to the Lippert-Mataga[10, 11] formalism (Eqs. 1 and 2) and considers the dependence of the fluorescence maxima and Stokes shifts on two solvent polarity functions, $F_1(\varepsilon,n)$ and $F_2(\varepsilon,n)$, respectively.

$$\nu_f = \nu_{f0} - \frac{2(\Delta\mu)^2}{hca^3}\left(\frac{\varepsilon-1}{2\varepsilon+1} - \frac{n^2-1}{2(2n^2+1)}\right) = \nu_{f0} - \frac{2(\Delta\mu)^2}{hca^3}F_1(\varepsilon,n) \quad (1)$$

$$\nu_a - \nu_f = \Delta\nu_{Stokes} = \frac{2(\Delta\mu)^2}{hca^3}\left(\frac{\varepsilon-1}{2\varepsilon+1} - \frac{n^2-1}{2n^2+1}\right) = \frac{2(\Delta\mu)^2}{hca^3}F_2(\varepsilon,n) \quad (2)$$

where ν_a and ν_F represent the wavenumbers of the absorption and fluorescence maxima, respectively, *c* is the speed of light in vacuum, *h* is Planck's constant, *a* the solute cavity radius, $\Delta\mu$ the dipole moment variation upon excitation, ε the dielectric constant of the medium and *n* the refractive index of the solvent.

Another way to analyze the Stokes displacement is to use Ravi and co-workers' formalism.[12] These authors interpret the data by using the solvent polarity parameter $E_T(30)$ proposed by Reichardt (Eqs. 3–5):[13]

$$E_T(30)\left(kcalmol^{-1}\right) = 2.8591\times10^{-3}\nu_a(cm^{-1}) \quad (3)$$

The normalized value of $E_T(30)$, E_T^N, is given by:

$$E_T^N = \frac{E_T(solvent) - E_T(TMS)}{E_T(water) - E_T(TMS)} = \frac{E_T(solvent) - 30.7}{63.1 - 30.7} \quad (4)$$

where TMS represents tetramethylsilane and $E_T(TMS) = 30.7$ kcal/mol, $E_T(water) = 63.1$ kcal/mol. Given these, the Stokes shift can be analyzed with the relation:

$$\nu_a - \nu_F = \Delta\nu_{Stokes} = 11307.6\left(\frac{\Delta\mu}{\Delta\mu_D}\right)^2\left(\frac{a_D}{a}\right)^3 E_T^N + const \quad (5)$$

where $\Delta\mu_D$ and a_D are the dipole moment variation upon excitation and the cavity radius of the pyridinium N-phenoxide betaine dye, respectively.

The Lippert-Mataga plots of the solvatochromic effect for compound **II**, considering both the fluorescence maximum and Stokes shift values (Eqs. 1 and 2), show a great deviation of the protic solvents from the expected linearity (Fig. 3). Analysing our data according to Eq. 5, *i.e.* considering the Stokes shift dependence on the normalized Reichardt parameter, E_T^N, also lead to large deviations from linearity of the values in protic solvents (Fig. 4).

In order to better evidence the relative contributions of solvent polarity and proticity, an analysis using the Kamlet-Taft (Eqs. 6 and 7)[14] and Catalán (Eqs. 8 and 9)[15] models was also performed.

$$\nu_f = \nu_{f,0} + p(\pi^* + d\delta) + a\alpha + b\beta \quad (6)$$

$$\Delta\nu_{Stokes} = \Delta\nu_{Stokes,0} + p(\pi^* + d\delta) + a\alpha + b\beta \quad (7)$$

$$\nu_f = \nu_{f,0} + pSPP + aSA + bSB \quad (8)$$

$$\Delta\nu_{Stokes} = \Delta\nu_{Stokes,0} + pSPP + aSA + bSB \quad (9)$$

In Eqs. 6 and 7, π^*, α and β represent parameters describing the polarity of the solvent, its capacity of acting as hydrogen bond donor (HBD) and hydrogen bond acceptor (HBA), respectively, and $d\delta$ is a correction for chlorinated solvents. Parameters SPP, SA and SB in Eqs. 8 and 9 have the same meaning. The differences between the two models consist in the values used for the solvent parameters, that is in the polarity scales. The parameters used in the correlations were taken from references 14 and 15. The values of *p*, *a* and *b* are obtained by multiple regression analysis and show the relative contribution of the three solvent properties. The results are included in Table 4 and

reflect the fact that solvent polarity, solvent HBD and solvent HBA abilities influence the spectral properties of compound **II** to similar extents. This is in agreement with the previously inferred hydrogen bonding interaction occurring in protic solvents and responsible for the emission at 400 nm. A check of the accuracy of the multiple regression analysis is made plotting the experimental fluorescence wavenumbers and Stokes shifts against the predicted ones obtained using the determined *p*, *a* and *b* values. The plots are displayed in Figs. 5 and 6. Good correlations between the experimental and calculated data are obtained for both models.

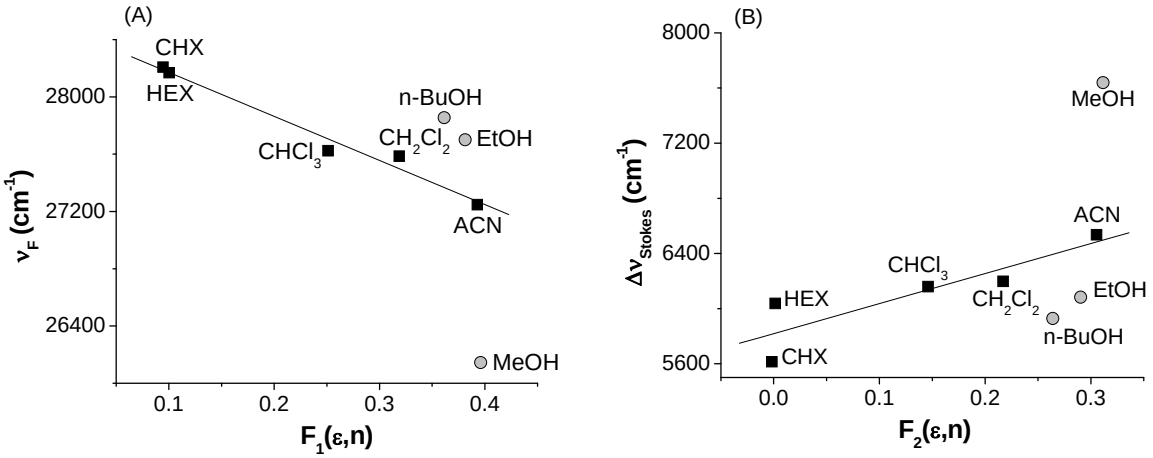

Fig. 3 – Lippert-Mataga dependences of the (A) fluorescence maxima, ν_F, and (B) Stokes shifts, $\Delta\nu_{Stokes}$, of compound **II** on the solvent polarity functions. Only the aprotic solvents were considered for the linear fits.

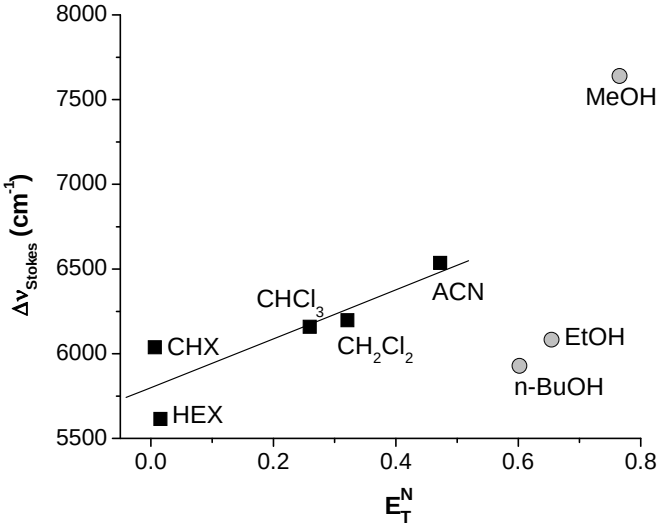

Fig. 4 – The dependence of the Stokes shift, $\Delta\nu_{Stokes}$, of compound **II** on the normalized Reichardt solvent parameter, E_T^N. Only the aprotic solvents were considered for the linear fits.

Table 4

The values of ν_0, *p*, *a* and *b* obtained using the Kamlet-Taft and Catalán models;
r^2 is the correlation coefficient of the plot of the experimental ν_F and $\Delta\nu_{Stokes}$ values against the ones predicted by the two models

Kamlet-Taft					
Eq.	*p*	*a*	*b*	ν_0 (cm^{-1})	r^2
(6)	–1940 (21%)	–3392 (36%)	4026 (43%)	28110	0.935
(7)	1658 (18%)	3353 (37%)	–4081 (45%)	5900	0.866
Catalán					
Eq.	*p*	*a*	*b*	ν_0 (cm^{-1})	r^2
(8)	–2701 (32%)	–3526 (41%)	2302 (27%)	29530	0.870
(9)	1928 (25%)	3520 (45%)	–2287 (30%)	4901	0.794

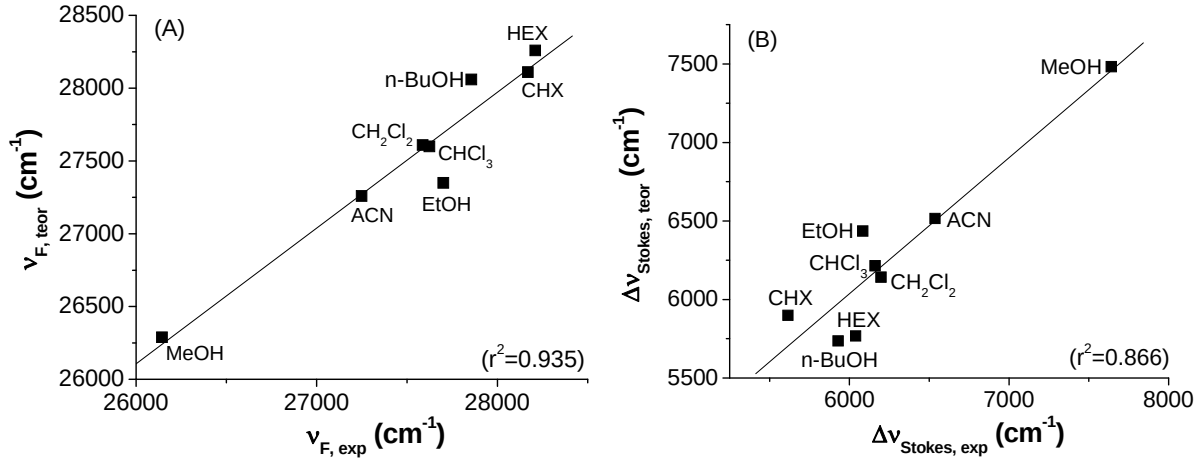

Fig. 5 – Plots of ν_F (A) and $\Delta\nu_{Stokes}$ (B) predicted using the Kamlet-Taft model *vs*. the experimental ones.

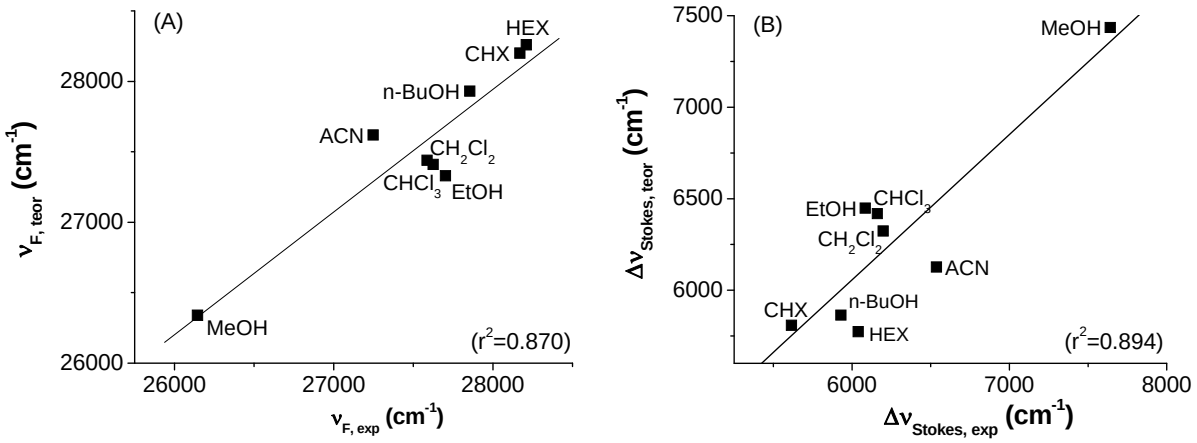

Fig. 6 – Plots of theoretical ν_F (A) and $\Delta\nu_{Stokes}$ (B) predicted using the Catalán model *vs*. the experimental ones.

Density functional theory (DFT) calculations

The large solvatochromic effect observed for compound **II** as compared to compound **I** suggests that the bromine substitution brings about a change in the nature of the first excited state, S_1. In order to get more information on the structural changes induced by the presence of the bromine atom, DFT calculations have been performed on both derivatives. Two parameters are relevant in characterizing their molecular structures, namely the planar/roof-shaped structure of the sulphone-substituted heteroring and the position of the bromine atom of the CH_2Br group. The roof-shaped structure of the phenoxathiinsulphone (Phx-SO_2) ring was previously discussed[16] and the structural parameters found for the totally optimized ground state are in agreement with the experimental ones.[17] The barrier for the inversion process calculated as the difference between a roof-shaped structure and a totally planar one was 0.53 kcal mol^{-1}.

In what concerns the position of the substituent, one of the first aspects taken into account was the determination of the barrier to rotation of the CH_2Br group in respect to the substituent–ring bond, *i.e.* the torsion angle, τ. The potential energy curve built considering for τ a step of 30 deg is displayed in Fig. 7 and led to a barrier to rotation of about 2.5 kcal mol^{-1}, reflecting the free rotation of the CH_2Br group. A similar treatment performed for the related compound, 2-CH_2Br-phenoxathiinsulphone, led to somewhat larger barrier to rotation values in the range 3.3–3.9 kcal mol^{-1}, depending on the atomic basis set used.[16]

A first check of the molecular orbitals calculations was made by comparing the experimental absorption spectra in the region of the excitation wavelength with the calculated ones. Considering the different possible positions of the CH_2Br group, *i.e.* the position of bromine in respect with the heteroring, a convolution of the spectra in CHX and MeOH, calculated for different τ values and weighed by the Boltzmann population

(determined from the calculated energies), was performed (Fig. 8). The averaged spectra match well the experimental ones in both solvents, the agreement being better in MeOH, 286 *vs.* 296 nm. Comparing the spectra of the different conformations, the values of $\tau = \pm 90$ deg lead to the best agreement with the experimental position of the absorption maximum, 290 nm *vs.* 296 nm.

For a better characterization of the first excited state S_1, the isodensity contours of the frontier molecular orbitals, *homo* and *lumo*, are displayed in Fig. 9.

In all derivatives, the sulphone group is not involved in the highest occupied molecular orbital. This is totally different from the case of phenoxathiin derivatives, for which *homo* is practically localized on the sulphur atom, explaining the donor character of the heteroring.[5] Concerning the *lumo* orbitals of the three sulphones, the unsubstituted Phx-SO_2 and derivatives **I** and **II,** we can see that this frontier orbital is practically identical in Phx-SO_2 and **I**, whereas it contains a large contribution from the bromine atom in **II**. This fact explains the similarity between the photophysical properties of Phx-SO_2 and **I**, and the different spectral behaviour of **II**. For **II**, a charge transfer is expected, directed from the heteroring towards the substituent, explaining the bathochromic shift observed in the fluorescence spectrum. These features are maintained, irrespective of the position of the CH_2Br group, meaning that during free rotation, the bromine atom is always involved in the formation of *lumo*.

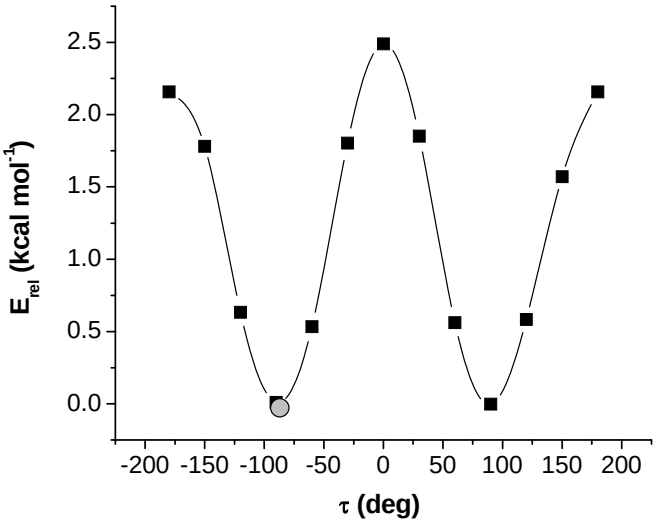

Fig. 7 – Potential energy curve built in respect to the torsion angle τ of the CH_2Br group of compound **II**. The absolute minimum energy point (total optimization) found at –87 deg is also depicted (in gray).

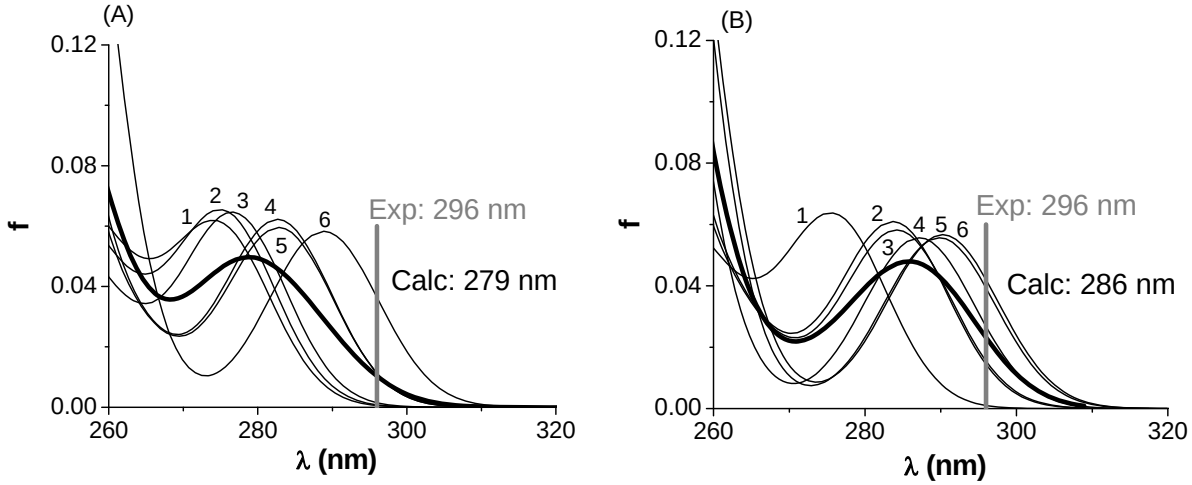

Fig. 8 – Averaged calculated electronic spectrum (in black, bold) of **II** in (A) CHX and (B) MeOH considering several positions of the CH_2Br group in respect with the heteroring. (A): τ (deg) = +30 (1), –150 (2), +150 (3), –60 (4), +60 (5) and –90 (6); (B): τ (deg) = 155 (1), –60 (2), +60 (3), +120 (4), +90 (5) and –90 (6); f stands for the oscillator strength of the transitions. The experimental positions of the absorption maxima in the two solvents are given in gray.

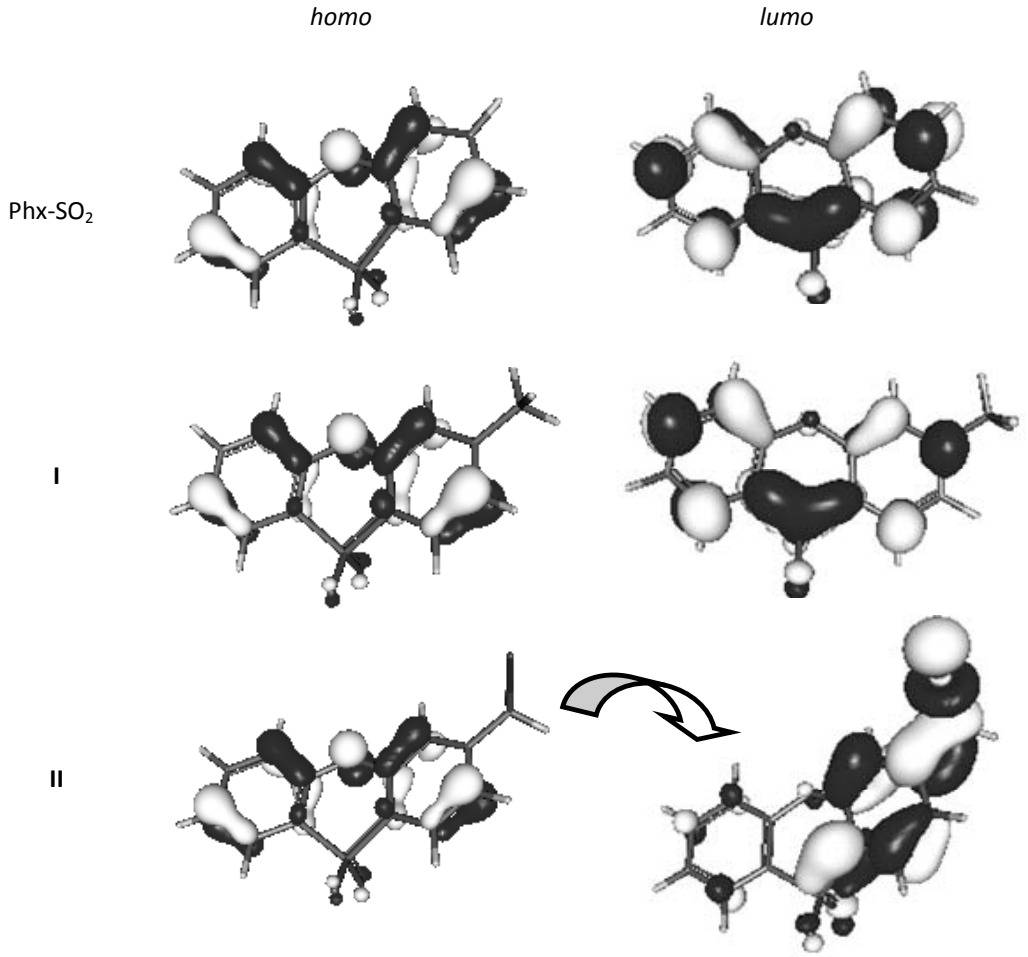

Fig. 9 – Isodensity contours of the frontier molecular orbitals (*homo* and *lumo*) of Phx-SO_2, **I** and **II**. The isodensity value is the same for all compounds (0.06 for *homo*, 0.04 for *lumo*).

In ground state, the substitution of one hydrogen atom of the CH_3 group with a bromine atom determines an increase of the positive Mulliken charge on the remaining two hydrogens from +0.17e to +0.23e. Due to the charge transfer from the heteroring to the substituent that occurs in the S_1 state, a more negative charge on bromine is expected and even larger positive charge density values on the two hydrogen atoms, thus explaining the solvent effect and comparative contributions of the HBD and HBA terms in the Kamlet-Taft analysis.

EXPERIMENTAL DATA AND COMPUTATIONAL DETAILS

Phenoxathiinsulphone was purchased from Fluka; derivatives **I** and **II** were synthesized as was previously described.[18] The fluorescence spectra were recorded on the JASCO FP-6300 spectrofluorimeter using solutions with absorbance below 0.1, in order to ensure the linear absorbance−concentration dependence and to avoid inner filter effects. The solvents were of spectroscopic grade, provided by Aldrich and Fluka and used without further purification. The fluorescence quantum yields were determined using quinine sulphate in 0.5 M sulphuric acid as standard, following the procedure described elsewhere.[19]

The calculations were performed by the Gaussian09 program[20] using the B3LYP[21] functional and the 6-31G(d) atomic basis set.[22] The solvent effect was considered in the frame of the polarisable continuum model.[23, 24] In the TDDFT calculations of the electronic spectra, ten excited states were taken into account. The UV spectra were plotted using the Gabedit 2.4.7 program.[25]

CONCLUSIONS

The fluorescence study of the two phenoxathiin-10,10-dioxide derivatives **I** and **II** shows the significant role of the substituent on the photophysical properties of this class of heterocycles. It was found that introducing a bromine atom in the methyl group determines a strong solvatochromic effect in the fluorescence spectrum and a deviation from linearity in protic solvents, as described by the Lippert-Mataga and Ravi models. The deconvolution of the fluorescence spectra of **II** reflects the presence of

two emitting species, one of them more enhanced in protic media. The analysis of the experimental data by the Kamlet-Taft and Catalán models supports this assumption. These results suggest the presence of a charge transfer excited state. The estimated quantum yields attest the previous observations on the more intense emissive properties in the presence of a substituent in position 3 as compared to position 2. The theoretical calculations support the presence of a charge transfer occurring in the excited state from the heteroring towards the CH_2Br group in position 3, explaining the difference in the solvent effect on the fluorescence spectra of **I** and **II.** This transfer does not occur in Phx-SO_2 and **I**, for which only a weak charge transfer within the cycle is observed.

REFERENCES

1. M. Hillebrand, O. Maior, V. E. Sahini and E. Volanschi, *J. Chem. Soc. B*, **1969**, 755-761.
2. M. Hillebrand, O. Maior and V. E. Sahini, *Rev. Roum. Chim.*, **1970**, *18*, 149-152.
3. I. Baciu, M. Hillebrand and V. E. Sahini, *J. C. S. Perkin II*, **1974**, 986-989.
4. I. A. Gad El-karim, *J. Mol. Struct: THEOCHEM*, **2010**, *945*, 17-22.
5. S. Ionescu, D. Gavriliu, O. Maior and M. Hillebrand, *J. Photochem. Photobiol. A: Chemistry*, **1999**, *124*, 67-73.
6. M. Ciureanu, M. Hillebrand and E. Volanschi, *J. Electroanal. Chem.*, **1992**, *322*, 221-232.
7. E. Constantinescu, M. Hillebrand, E. Volanschi, M. Andrei, G. Ivanescu and O. Maior, *J. Electroanal. Chem.*, **1995**, *395*, 211-220.
8. L. Preda, V. Lazarescu, M. Hillebrand and E. Volanschi, *Electrochim. Acta*, **2006**, *51*, 5587-5595.
9. E. Volanschi, S. H. Suh and M. Hillebrand, *J. Electroanal. Chem.*, **2007**, *602*, 181-188.
10. A. Vlahovici, H. Ofenberg, L. Cires, A. Pollet and A. Lablache-Combier, *J. Lumin.*, **1994**, *62*, 227-236.
11. W. Verbouwe, L. Viaene, M. Van der Auweraer, F. C. De Schryver, H. Masuhara, R. Pansu, and J. Faure, *J. Phys. Chem. A*, **1997**, *101*, 8157-8165.
12. M. Ravi, A. Samanta and T. P. Radhakrishnan, *J. Phys. Chem.*, **1994**, *98*, 9133-9136.
13. C. Reichardt, "Solvents and Solvent Effects in Organic Chemistry", Wiley-VCH: Weinheim, 2003, p. 354.
14. M. J. Kamlet, J. M. Abboud, M. H. Abraham and R. W. Taft, *J. Org. Chem.*, **1983**, *48*, 2877-2887.
15. J. Catalán, "Handbook of Solvents", G. Wypych (Ed.) ChemTech Publishing, Toronto, 2001, p. 583.
16. R. Sandu, C. Tablet and M. Hillebrand, *J. Incl. Phenom. Macrocycl. Chem.*, **2013**, *77*, 183-193.
17. A. D. Hendsbee, J. D. Masuda and A. Piorko, *Acta Cryst.*, **2011**, *C67*, m351–m354.
18. G. Vasiliu and O. Maior, *An. Univ. Bucuresti Chimie*, **1964**, *13*, 103-111.
19. B. Valeur, "Molecular Fluorescence. Principles and Aplications", Wiley-VCH: Weinheim, Germany, 2002, p. 155.
20. Gaussian 09, Revision C.01, M. J. Frisch, G. W. Trucks, H. B. Schlegel, G. E. Scuseria, M. A. Robb, J. R. Cheeseman, G. Scalmani, V. Barone, B. Mennucci, G. A. Petersson, H. Nakatsuji, M. Caricato, X. Li, H. P. Hratchian, A. F. Izmaylov, J. Bloino, G. Zheng, J. L. Sonnenberg, M. Hada, M. Ehara, K. Toyota, R. Fukuda, J. Hasegawa, M. Ishida, T. Nakajima, Y. Honda, O. Kitao, H. Nakai, T. Vreven, J. A. Montgomery, Jr., J. E. Peralta, F. Ogliaro, M. Bearpark, J. J. Heyd, E. Brothers, K. N. Kudin, V. N. Staroverov, R. Kobayashi, J. Normand, K. Raghavachari, A. Rendell, J. C. Burant, S. S. Iyengar, J. Tomasi, M. Cossi, N. Rega, J. M. Millam, M. Klene, J. E. Knox, J. B. Cross, V. Bakken, C. Adamo, J. Jaramillo, R. Gomperts, R. E. Stratmann, O. Yazyev, A. J. Austin, R. Cammi, C. Pomelli, J. W. Ochterski, R. L. Martin, K. Morokuma, V. G. Zakrzewski, G. A. Voth, P. Salvador, J. J. Dannenberg, S. Dapprich, A. D. Daniels, O. Farkas, J. B. Foresman, J. V. Ortiz, J. Cioslowski and D. J. Fox, Gaussian, Inc., Wallingford CT, 2009.
21. A. D. Becke, *J. Chem. Phys.*, **1993**, *98*, 5648-5652; P. J. Stephens, F. J. Devlin, C. F. Chabalowski and M. J. Frisch, *J. Phys. Chem.*, **1994**, *98*, 11623-11627.
22. W. J. Hehre, R. Ditchfield and J. A. Pople, *J. Chem. Phys.*, **1972**, *56*, 2257-2261; P. C. Hariharan and J. A. Pople, *Theor. Chim. Acta,* **1973**, *28*, 213-222.
23. B. Mennucci, C. Cappelli, R. Cammi and J. Tomasi, *Chirality*, **2011**, *23*, 717-729.
24. J. Tomasi, B. Mennucci and R. Cammi, *Chem. Rev.*, **2005**, *105*, 2999-3093.
25. A. R. Allouche, *J. Comput. Chem.*, **2011**, *32*, 174-182.